Available online at www.sciencedirect.com

ScienceDirect

IFAC Papers Online CONFERENCE PAPER ARCHIVE

IFAC-PapersOnLine 48-1 (2015) 029–034

Efficient DQMOM for Multivariate Population Balance Equations and Application to Virus Replication in Cell Cultures

R. Dürr [*,⋆] **T. Müller** [*] **A. Kienle** [*,**]

[*] *Otto-von-Guericke-Universität, 39106 Magdeburg, Germany*
[**] *Max-Planck-Institut für Dynamik komplexer technischer Systeme, 39106 Magdeburg, Germany*

Abstract:
Population balances play an important role in process and bioprocess engineering. They represent PDEs which are often multidimensional. The numerical solution of these is quite challenging in particular for high dimensional problems. For this reason the distribution dynamics are usually represented by the respective moments. As the corresponding dynamic moment equations can only be computed in a closed form under strict assumptions, approximate moment methods have to be applied. However, existing techniques can not be implemented efficiently for high dimensional problems. In this manuscript an efficient implementation of the Direct Quadrature Method of Moments (DQMOM) is derived using monomial cubature rules. Furthermore, application is demonstrated for a five dimensional PBE which is based on a single cell model for viral replication in cell cultures. The algorithm is used to analyze the effects of different model assumptions on the overall dynamics.

Keywords: Heterogeneity, Population Balance Modeling, Multidimensional Partial Differential Equations, Direct Quadrature Method of Moments, Monomial Cubatures, Virus Replication, Cell Cultures

1. INTRODUCTION

Multidimensional population balances can be found in many applications from process and bioprocess engineering. Typical examples are shape evolution in crystallization processes (Liu et al., 2010) and the characterization of intracellular dynamics of cell cultures in bioprocess engineering (Villadsen et al., 2011). Their dynamics can be described conveniently using the framework of population balance equations (PBEs) (Ramkrishna, 2000)

$$\frac{\partial n(t,\mathbf{x})}{\partial t} + \sum_{k=1}^{d} \frac{\partial}{\partial x_k} \left\{ h_k(t,\mathbf{x},\mathbf{c})\, n(t,\mathbf{x}) \right\} = B(t,n,\mathbf{x},\mathbf{c}) - D(\mathbf{x},\mathbf{c},t)\, n(t,\mathbf{x})\,. \tag{1}$$

The resulting partial differential equations (PDEs) specify the dynamics of the number density distribution $n(t,\mathbf{x})$ with respect to the vector of internal coordinates $\mathbf{x} = [x_1,\ldots,x_d]$. The rates h_k define the advection in direction of internal coordinates while the right hand side comprises sources and sinks. In general, the PBE for the so called dispersed phase is coupled to a system of ODEs characterizing the dynamics of the continuous phase vector $\mathbf{c} = [c_1,\ldots,c_{d_e}]$

$$\frac{d\mathbf{c}}{dt} = P\,(\mathbf{c}_{in} - \mathbf{c}) + \mathbf{f}(\mathbf{c},n) \tag{2}$$

with P being the dilution rate and $\mathbf{f}$ the integral exchange with the dispersed phase. Population balance equations are rarely solvable analytically. Most numerical solution techniques can be assigned to one of the following classes. Monte Carlo (MC) methods are based on the solution of a corresponding stochastic problem formulation (Zhao et al., 2007). Here, the number of simulated particles has to be sufficiently high to come up with reliable results. In consequence, for multidimensional problems the application of MC techniques involves high computational costs. In discretization-based algorithms like finite volume methods (Ma et al., 2002) the space of internal coordinates is discretized and a large set of ODEs is solved instead of a PDE. Like MC methods, discretization-based methods suffer from large numerical effort when being applied to multidimensional problems. In contrast to these techniques moment methods rely on specific integral quantities of the distribution, the so called moments. These moments are defined as

$$m_{l_1,\ldots,l_d} = \int_{\mathbf{X}} x_1^{l_1} \ldots x_d^{l_d}\, n(t,\mathbf{x})\, d\mathbf{x}\,. \tag{3}$$

They are directly related to important integral properties of the distribution function like overall number of particles, overall particle surface and overall particle mass. The dynamic moment equations can be derived from the PBE easily

⋆ Correspondence to: R. Dürr, Otto-von-Guericke-Universität, Universitätsplatz 2, 39106 Magdeburg, Germany (e-mail: robert.duerr@ovgu.de)

2405-8963
Peer review under responsibility of International Federation of Automatic Control.
10.1016/j.ifacol.2015.05.045

$$\frac{d}{dt}m_{l_1,\dots,l_d} = -\sum_{k=1}^{d}\int_{\mathbf{X}} x_1^{l_1}\dots x_d^{l_d}\,\frac{\partial}{\partial x_k}\left\{h_k\,n\right\}d\,\mathbf{x} \qquad (4)$$
$$+\int_{\mathbf{X}} x_1^{l_1}\dots x_d^{l_d}(B-D\,n)\,d\mathbf{x}\,.$$

where the right hand side has to be expressed in terms of moments. Computation of the dynamics using a closed set of equations is only possible under strict assumptions. However, an approximate closure can be found using approximate moment methods like the Quadrature Method of Moments (QMOM) as presented by McGraw (1997) or the Direct Quadrature Method of Moments (DQMOM) as described by Marchisio and Fox (2005). These methods have been applied to many processes governed by one- or two-dimensional PBEs and are specifically suitable in combination with CFD simulations. Multivariate extensions have been developed (e.g. Buffo et al., 2013) but are rarely applied to PBEs with more than two internal coordinates. This is mainly due to two problems. First, application of QMOM or DQMOM includes the solution of possibly ill conditioned nonlinear (QMOM) or linear (DQMOM) equation systems. This is further complicated in the multidimensional setting. A second problem arises from the choice of abscissas and weights for the approximation of the integral (3). Here, a good trade-off between accuracy and numerical effort has to be found.

In the following, an alternative method is presented which can be implemented efficiently, even for large dimensional problems. Note, that this approach can be interpreted as a generalzation of a recently presented algorithm of Dürr and Kienle (2014). Furthermore, the algorithm is applied to a structured and segregated model describing virus replication in cell culture.

2. APPROXIMATION OF MOMENTS USING THE DIRECT QUADRATURE METHOD OF MOMENTS

The Direct Quadrature Method of Moments was introduced by Marchisio and Fox (2005). It is assumed that the integrals of the number distribution function can be approximated as the following:

$$\int_{\mathbf{X}} f(\mathbf{x})\,n\,d\,\mathbf{x} \approx \sum_{\alpha=1}^{n_\alpha} w_\alpha(t)\,f(\mathbf{x}_\alpha(t)) = \sum_{\alpha=1}^{n_\alpha} w_\alpha\,f_\alpha \qquad (5)$$

with w_α the weight and $\mathbf{x}_\alpha$ the corresponding abscissa. Thus moments (3) are approximated by

$$m_{l_1,\dots,l_d} = \int_{\mathbf{X}} x_1^{l_1}\dots x_d^{l_d}\,n\,d\mathbf{x} = \sum_{\alpha=1}^{n_\alpha} w_\alpha\,x_{1,\alpha}^{l_1}\dots x_{d,\alpha}^{l_d}\,. \quad (6)$$

As a consequence of effects like particle growth, the distribution and its corresponding moments undergo changes during the process. Instead of describing the evolution of any moment the main idea of DQMOM is to track the evolution of abscissas and weights directly. Introducing

$$\frac{d\,w_\alpha}{dt} = a_\alpha\,, \qquad \frac{d\,w_\alpha\,x_{i,\alpha}}{dt} = b_{i,\alpha} \qquad (7)$$

for the dynamics of the weights and abscissas the following equation for an arbitrary moment as defined in (3) can be derived from the moment dynamics (4)

$$\sum_{\alpha=1}^{n_\alpha}\left\{(1-\sum_{k=1}^{d}l_k)\,x_1^{l_1}\dots x_d^{l_d}\,a_\alpha + \right. \qquad (8)$$
$$\left.\begin{bmatrix} l_1\,b_{1,\alpha}\\ \vdots\\ l_d\,b_{d,\alpha}\end{bmatrix}^T\cdot\begin{bmatrix} x_{1,\alpha}^{l_1-1}x_{2,\alpha}^{l_2}\dots x_{d,\alpha}^{l_d}\\ \vdots\\ x_{1,\alpha}^{l_1}x_{2,\alpha}^{l_2}\dots x_{d,\alpha}^{l_d-1}\end{bmatrix}\right\} = S_{\mathbf{x}}^{\mathbf{l}}\,.$$

Here $S_{\mathbf{x}}^{\mathbf{l}}$ contains the right hand hand side of (4) and can also be approximated using (5). In general, one has to evaluate the equation for $n_\alpha\,(d+1)$ distinct moments to come up with a linear system which has to be solved for the unknown expressions $\mathbf{a}_\alpha$ and $\mathbf{b}_{k,\alpha}$.

$$A\cdot\begin{bmatrix}\mathbf{a}\\ \mathbf{b}\end{bmatrix} = \mathbf{S} \qquad (9)$$

Depending on the choice of moments different solutions can be obtained. It is well known that A can become ill-conditioned depending on the choice of moments, in particular for a large n_α and d.

However, if $B = 0$, a solution can be derived very effectively by using only the zeroth and first order moments of the distribution function. For the zeroth order moment (i.e. $l_1 = \dots = l_d = 0$) (8) is simplified to

$$\sum_{\alpha=1}^{n_\alpha} a_k \approx -\sum_{\alpha=1}^{n_\alpha} w_\alpha D_\alpha\,. \qquad (10)$$

Comparing the coefficients yields the resulting ODEs for the dynamics of weights

$$\frac{dw_\alpha}{dt} = -w_\alpha D_\alpha\,. \qquad (11)$$

In the next step (8) is solved for each first order moment (i.e. $l_i = 1\,,\ l_j = 0\,,\ i,j = 1,\dots,5\,,\ i \neq j$). The resulting equation is given by

$$\sum_{\alpha=1}^{n_\alpha} b_{i,\alpha} \approx \sum_{\alpha=1}^{n_\alpha} w_\alpha\,(h_{i,\alpha} - x_{i,\alpha}\,D_\alpha)\,. \qquad (12)$$

As in the previous case rearranging and comparison of the coefficients yields

$$b_{i,\alpha} = w_\alpha\,(h_{i,\alpha} - x_{i,\alpha}\,D_\alpha)\,. \qquad (13)$$

Combination of (7),(11) and (13) yields the dynamics of the abscissas

$$\frac{dx_{i,\alpha}}{dt} = h_{i,\alpha}\,. \qquad (14)$$

By using both derived equations the temporal evolution of abscissas and weights can be calculated directly. The abscissas move along the characteristic curves of (1) and the overall algorithm is equivalent to the one presented in Dürr and Kienle (2014).

3. CHOICE OF ABSCISSAS

In the previous section dynamic equations for weights and abscissas have been derived. However, the actual choice of abscissas for the approximation (5) is still unclear. Obviously, this is a crucial point with respect to the numerical effort and accuracy of the whole approximate moment method. The abscissas and weights are chosen based on the initial distribution. There are numerous contributions that present different rules for the numerical approximation of multivariate integrals as summarized in Stroud (1971). In general, these cubatures can be divided into two main

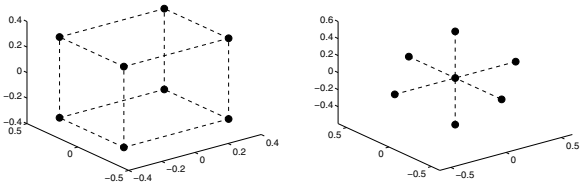

Fig. 1. *Abscissas for $d = 3$: PG3 (left) and NP3 (right)*

classes. Product formulas are multivariate extensions of one-dimensional quadrature formulas. Here, the size of the abscissa set increases exponentially with the dimension of the problem. In contrast, when using non-product formulas, a special shape of the initial distribution is assumed. In this case the abscissa set increases polynomially with the number of internal coordinates. Consequently, non-product rules do not suffer from the curse of dimensionality as significantly as product formulas.

In the following, the initial condition is assumed to be a multidimensional Gaussian normal distribution

$$n(t=0,\mathbf{x}) = \mathcal{N}(\mu, \mathbf{\Sigma}) \tag{15}$$

with mean μ and covariance-matrix $\mathbf{\Sigma}$. In this case, particularly efficient non-product rules can be found. The first non-product rule is the square-root sigma-point rule as presented for example in van der Merwe (2004). It is a third degree monomial cubature (NP3) which is used extensively in the core routine of the Unscented Kalman Filter. The numerical effort by means of total number of abscissas is given by $n_\alpha = 2\,d + 1$. Hence, the size of the abscissa set scales linearly with dimension d. Two additional cubature formulas will be applied and compared to NP3 in the following example. The first one is a fifth degree monomial cubature formula (NP5) as described in Stroud (1971). Here, the overall number of abscissas increases quadratically with the dimension: $n_\alpha = 2\,n^2 + 1$. Furthermore, a third degree Cartesian product Gauss formula (PG3) will be applied. It can also be found in Stroud (1971). Here, the overall number of abscissas is given by $n_\alpha = 2^d$ and thus, the size of the abscissa set scales exponentially with the dimension. In Fig. 1 the general distribution of the abscissas for PG3 and NP3 for $d = 3$ can be seen.

4. A STRUCTURED POPULATION BALANCE MODEL FOR VIRUS REPLICATION IN CELL CULTURES

Influenza vaccine production in mammalian cell cultures constitutes a great example of a biotechnological process that is characterized by a heterogeneous population of cells. Besides the obvious discrimination between uninfected and infected cells, a further differentiation of the subpopulation of infected cells allows for the consideration of the innate cell-to-cell variability and, thereby, facilitates the explanation of characteristic dynamic phenomena of the overall process. This has been shown recently by Dürr et al. (2012) and Müller et al. (2013) for the production of different influenza A virus strains. Therein infected cells have been differentiated with respect to the intracellular amount of accumulated viral nucleoprotein NP, which was measured via flow cytometry. Although the corresponding non-structured, segregated model is able to reproduce the essential dynamic effects, its predictive capacity is limited. In order to improve this situation a more detailed description of the intracellular viral replication kinetics seems appropriate.

As mentioned earlier, the solution of the emerging high dimensional PDEs is challenging. Our aim is to use the DQMOM in combination with special cubature rules to efficiently solve a more detailed intracellular viral replication mechanism which is taken from Haseltine et al. (2005) and integrated in a corresponding multidimensional PBE. In Fig. 2 the basic intracellular reaction scheme is depicted. Upon infection of an uninfected cell viral genomic nucleic acid $[gen]$ is inserted. In the next step template viral nucleic acid $[tem]$ is produced from the viral genome. In turn, these templates are used for the production of viral genome and viral structural protein $[str]$. Virus progeny are assembled from structural protein and viral genome in order to be released into the medium. Furthermore, it is assumed, that the production of templates and structural protein is catalyzed by the intracellular enzymes v_1 and v_2.

The intracellular states

$$\mathbf{x} = ([tem],\,[gen],\,[str],\,[v_1],\,[v_2])^T \tag{16}$$

directly translate to internal coordinates of a corresponding PBE which characterizes the dynamics of the number density distribution of infected cells

$$\begin{aligned}\frac{\partial n(t,\mathbf{x})}{\partial t} &= -\sum_{k=1}^{5} \frac{\partial}{\partial x_k}\left\{h_k(t,\mathbf{x},\mathbf{c})\, n(t,\mathbf{x})\right\} \\ &+k_{inf}\, U_C\, V\, \mathcal{N}_{inf}(\mu,\mathbf{\Sigma}) - k_{cd,I_c}\, n(t,\mathbf{x})\,.\end{aligned} \tag{17}$$

The vector of advection velocities results from balancing of the compounds on the single cell level (Villadsen et al., 2011):

$$\mathbf{h} = \begin{bmatrix} k_1[v_1][gen] \\ k_3[tem] - k_1[gen][v1] - k_5[gen][str] \\ k_2[tem][v_2] - k_4[str] - k_5[gen][str] \\ f_{v_1} \\ f_{v_2} \end{bmatrix}. \tag{18}$$

Here, f_{v_1} and f_{v_2} are the enzyme production/degeneration rates. Newly infected cells are generated by infection of uninfected cells U_c by free virions V. It is assumed that infected cells are spawned into the space of internal properties according to a normal distribution $N_{inf}(\mu, \mathbf{\Sigma})$ and infected cells die with rate k_{cd}. The dynamics of the uninfected cells and the free virions are given by

$$\begin{aligned}\frac{d\,U_C}{d\,t} &= -k_{inf}\, U_C\, V + k_{gro} - k_{cd,U_C} U_C \\ \frac{d\,V}{d\,t} &= \int_{\mathbf{X}} r_{rel}(\mathbf{x})\, n\, d\mathbf{x} - k_{inf}\, U_C\, V\, - k_{deg}\, V\end{aligned} \tag{19}$$

with the virus release rate depending on the intracellular composition of each cell

$$r_{rel}(\mathbf{x}) = k_5\,[gen]\,[str]\,. \tag{20}$$

5. RESULTS

5.1 Implementation Issues

For the numerical solution the dynamic equations for the whole set of weights (11) and abscissas (14) have to

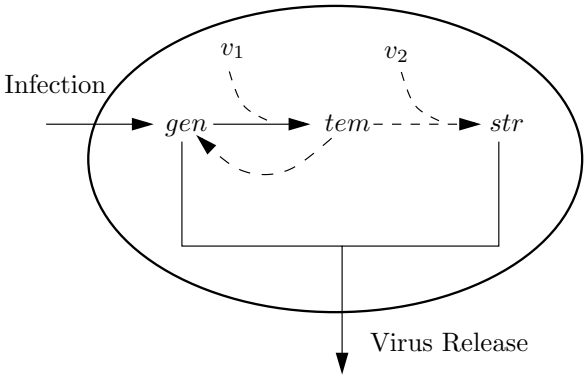

Fig. 2. *Single cell scheme for viral replication*

be applied simultaneously to the ODEs (19). This also involves the simultaneous solution of (9).

However, for this special type of example an even more effective solution can be implemented. The main idea is the following: instead of the full problem (18) a series of subproblems is solved. Each subproblem corresponds to

$$\begin{aligned}\frac{\partial \widetilde{n}(\xi,\mathbf{x})}{\partial \xi} &= -\sum_{k=1}^{5} \frac{\partial}{\partial x_k}\left\{h_k(\xi,\mathbf{x})\,\widetilde{n}(\xi,\mathbf{x})\right\} \\ &\quad - k_{cd,I_c}\,\widetilde{n}(\xi,\mathbf{x}) \\ \widetilde{n}(\xi=0,\mathbf{x}) &= k_{inf}\,U_C(t)\,V(t)\,\mathcal{N}_{inf}\,.\end{aligned} \tag{21}$$

Thus, the overall virus release is given by

$$\begin{aligned}R_{rel}(t) &= \int_{\mathbf{X}} r_{rel}(\mathbf{x})\,n(t,\mathbf{x})\,d\mathbf{x} \\ &= \int_0^t \int_{\mathbf{X}} r_{rel}(\mathbf{x})\,\widetilde{n}(\xi,\mathbf{x})\,d\mathbf{x}\,d\xi\,.\end{aligned} \tag{22}$$

Approximate computation of this and other integrals or moments for each subproblem can be performed efficiently using (11) and (14) in combination with monomial cubatures. Furthermore, as the intracellular kinetics (18) are decoupled from extracellular dynamics, the characteristic curves on which the abscissas are moving, are the same for each subproblem. Thus, the approximate evolution of moments or other integrals can be computed once for a scaled initial condition and be used further for the computation of the extracellular dynamics similar to the method described by Haseltine et al. (2008).

5.2 Scenario I: No enzyme degradation

In a first scenario it is assumed that there is no enzyme degradation. For this reason

$$f_{v_1} = f_{v_2} = 0 \tag{23}$$

and, thus, the intracellular levels of v_1 and v_2 are constant for each cell.

The resulting system is solved with the previously described procedure using the three introduced cubature formulas. Simulations show that all cubature rules produce nearly the same results. As an example, in Fig. 3 overall

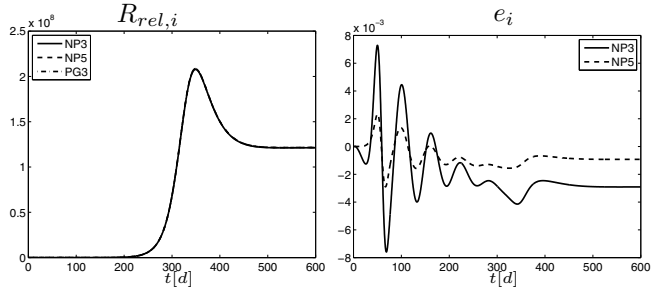

Fig. 3. *Comparison of virus release rates for different cubatures*

viral release rates $R_{rel,i}$ for the three rules and their relative differences are shown using PG3 as a reference

$$e_i = \frac{R_{rel,i} - R_{rel,PG3}}{R_{rel,PG3}}\,. \tag{24}$$

It can be seen that no significant error exists. For this reason cubature rule NP3 is used in the following as it has the lowest computational cost.

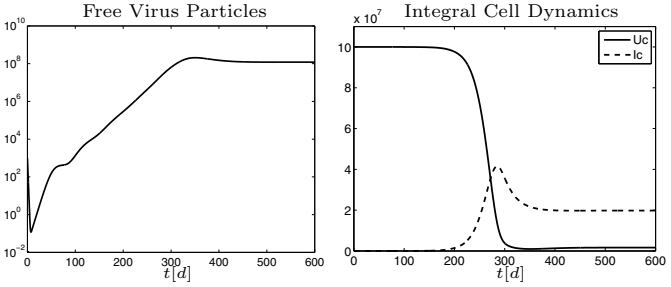

Fig. 4. *Viral and cell dynamics without enzyme degradation*

In Fig. 4 the resulting concentration of free virions and the overall number of cells is depicted. Initially, free virus particles attach to uninfected cells and infect them. Note, that the overall virus concentration stays low until a significant number of infected cells starts to produce viral components in a sufficiently high amount to facilitate the release of new virus particles. Afterwards, the virus concentration increases exponentially until the production slows down again and settles at a steady state as soon as the continuous supply and infection of uninfected cells as well as the death of infected cells are in balance.

In Fig. 5 the means and variances for the intracellular compounds

$$\mu_i = \frac{\int_{\mathbf{X}} x_i\,n\,d\mathbf{x}}{\int_{\mathbf{X}} n\,d\mathbf{x}} \qquad var_i = \frac{\int_{\mathbf{X}} x_i^2\,n\,d\mathbf{x}}{\int_{\mathbf{X}} n\,d\mathbf{x}} - \mu_i^2$$

are depicted. These oscillate for the first 200 days as several waves of viral infection follow in succession. Note, that due to the scale of the ordinate oscillations of the variances are not always visible. After about 200 days the continuous release of free virus particles causes a rapid decline of the number of uninfected cells and a simultaneous incline of the number of infected cells in order to reach a steady state after 400 days.

5.3 Scenario II: Degradation of intracellular enzymes

The second scenario features a degradation of the enzymes after infection. It is assumed, that upon infection cells

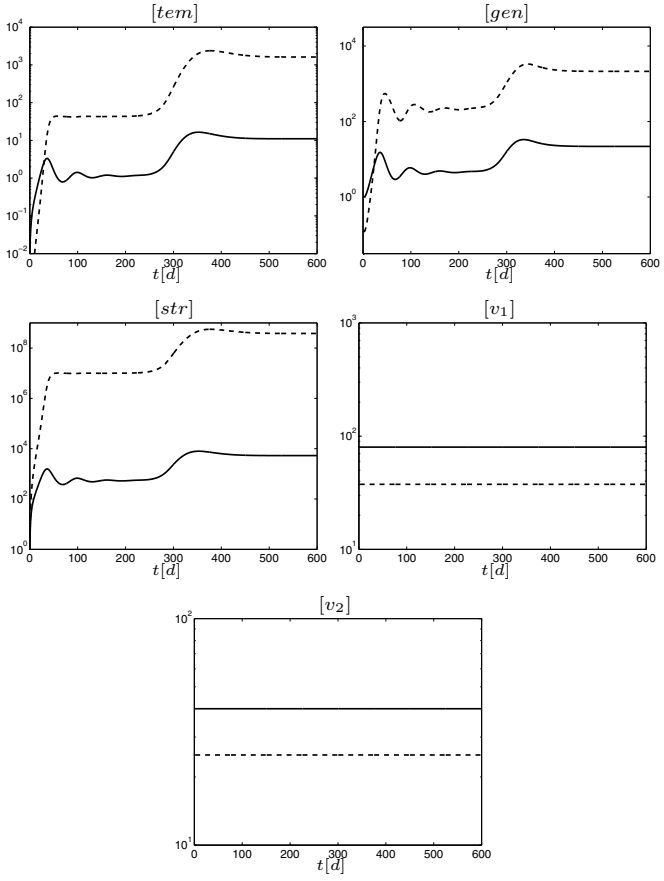

Fig. 5. *Dynamics of means (solid) and variances (dashed) w.r.t. intracellular coordinates without enzyme degradation*

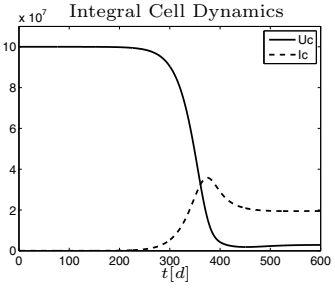

Fig. 6. *Cell dynamics with enzyme degradation*

lose their ability to sustain proper conditions for virus replication as they suffer from virus induced stress. This is expressed by a decreased capability to produce virus particles due to the loss of enzyme functionality:

$$f_{v_1} = -a_1 v_1 \,, \quad f_{v_2} = -a_2 v_2 \,. \tag{25}$$

In Fig. 6 and 7 the temporal change of the concentrations of uninfected and infected cells as well as free virus particles are shown, respectively. Due to enzyme degradation virus release proceeds at a lower rate. In consequence, the distinctive drop of the number of uninfected cells occurs at a later time and the steady state is reached later, too. This is mirrored by the dynamics of the intracellular components (see Fig. 8). The mean and variance of the intracellular content of structural protein is decreased and the variance of the intracellular content of viral genome

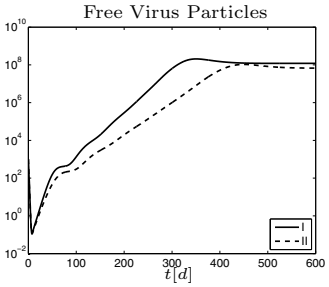

Fig. 7. *Comparison of virus dynamics without (solid) and with enzyme degradation (dashed)*

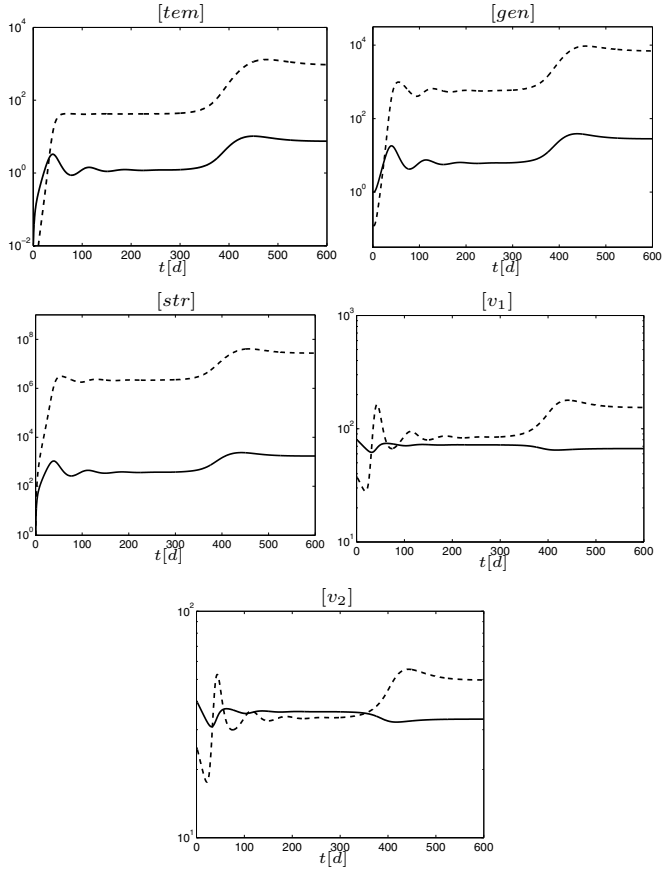

Fig. 8. *Dynamics of means (solid) and variances (dashed) w.r.t. intracellular coordinates with enzyme degradation*

is increased in comparison to the first scenario without enzyme degradation.

6. SUMMARY AND OUTLOOK

An effective and robust method for approximate computation of moments for multidimensional PBEs was presented. The algorithm is based on DQMOM. Furthermore, the technique can be implemented efficiently even for higher dimensional problems by using non-product cubature formulas. In contrast to product formulas these do not suffer from the curse of dimensionality up to a certain degree. Our method was applied to a five dimensional PBE describing viral replication in cell culture. It was shown, that the algorithm is suitable for analyzing the effects of resource limitations on important states like the overall number of released virus particles.

In the future, this efficient moment approximation algorithm will be applied to a more detailed model of influenza virus replication (see, e.g., Heldt et al., 2012), which describes intracellular dynamics much more in depth than the model presented here. By using the presented technique one is enabled to analyze the effects of intracellular enzyme degradation, resource limitations (e.g. Zhdanov, 2009) etc. on a macroscopic level in order to predict the final virus yield, which is most desirable in influenza vaccine production. In addition, the possibility of direct comparison with flow cytometric measurements of several intracellular components is provided.

Furthermore, the technique itself will be extended to deal with other particulate effects like agglomeration or non-Gaussian initial conditions.

ACKNOWLEDGEMENTS

The authors gratefully acknowledge the funding of this work by the German Federal Ministry of Science and Education (Bundesministerium für Bildung und Forschung - BMBF) as part of the "e:Bio" - project "CellSys" (grant number 031 6189 A).

REFERENCES

Buffo, A., Vanni, M., Marchisio, D., and Fox, R. (2013). Multivariate quadrature-based moments methods for turbulent polydisperse gasliquid systems. *International Journal of Multiphase Flow*, 50(0), 41 – 57.

Dürr, R. and Kienle, A. (2014). An efficient method for calculating the moments of multidimensional growth processes in population balance systems. *The Canadian Journal of Chemical Engineering*, 92, 2088–2097.

Dürr, R., Müller, T., Isken, B., Schulze-Horsel, J., Reichl, U., and Kienle, A. (2012). Distributed modeling and parameter estimation of influenza virus replication during vaccine production. In *Proceedings to 7th Vienna International Conference on Mathematical Modelling - MATHMOD 2012*, 320–325.

Haseltine, E.L., Rawlings, J.B., and Yin, J. (2005). Dynamics of viral infections: incorporating both the intracellular and extracellular levels. *Computers & Chemical Engineering*, 29(3), 675 – 686.

Haseltine, E.L., Yin, J., and Rawlings, J.B. (2008). Implications of decoupling the intracellular and extracellular levels in multi-level models of virus growth. *Biotechnology & Bioengineering*, 101(4), 811–820.

Heldt, S.F., Frensing, T., and Reichl, U. (2012). Modeling the intracellular dynamics of influenza virus replication to understand the control of viral rna synthesis. *Journal of Virology*, 86(15), 7806–7817.

Liu, J.J., Ma, C.Y., Hu, Y.D., and Wang, X.Z. (2010). Modelling protein crystallisation using morphological population balance models. *Chemical Engineering Research and Design*, 88(4), 437 – 446.

Ma, D.L., Tafti, D.K., and Braatz, R.D. (2002). High-resolution simulation of multidimensional crystal growth. *Industrial & Engineering Chemistry Research*, 41(25), 6217–6223.

Marchisio, D.L. and Fox, R.O. (2005). Solution of population balance equations using the direct quadrature method of moments. *Journal of Aerosol Science*, 36(1), 43 – 73.

McGraw, R. (1997). Description of aerosol dynamics by the quadrature method of moments. *Aerosol Science and Technology*, 27(2), 255–265.

Müller, T., Dürr, R., Isken, B., Schulze-Horsel, J., Reichl, U., and Kienle, A. (2013). Distributed modeling of human influenza a virus-host cell interactions during vaccine production. *Biotechnology and Bioengineering*, 110(8), 2252–2266.

Ramkrishna, D. (2000). *Population Balances: Theory and Applications to Particulate Systems in Engineering*. Academic Press, San Diego.

Stroud, A. (1971). *Approximate Calculation of Multiple Integrals*. Prentice-Hall, Englewood Cliffs, N.J., Englewood Cliffs, N.J.

van der Merwe, R. (2004). *Sigma-Point Kalman Filters for Probablilistic Inference in Dynamic State-Space Models*. Ph.D. thesis, Oregon Health & Science University.

Villadsen, J., Nielsen, J., and Liden, N. (2011). *Bioreaction Engineering Principles*. Springer Science & Business Media, Heidelberg, 3 edition.

Zhao, H., Maisels, A., Matsoukas, T., and Zheng, C. (2007). Analysis of four monte carlo methods for the solution of population balances in dispersed systems. *Powder Technology*, 173(1), 38 – 50.

Zhdanov, V.P. (2009). Intracellular viral kinetics limited by the supply of amino acids for synthesis of viral proteins. *Biosystems*, 97(2), 117–120.